Q. J. R. Meteorol. Soc. (1998), **124**, pp. 2417–2434

Radar estimates of rainfall rates at the ground in bright band and non-bright band events

By T. J. SMYTH* and A. J. ILLINGWORTH
University of Reading, UK

(Received 4 September 1997; revised 23 March 1998)

SUMMARY

The major error in estimating precipitation rates at the ground from radar arises from the change in radar reflectivity (Z) with height. In stratiform precipitation Z rises in the 'bright band', where the snow is melting, and then falls steeply in the dry ice above. In regions of vigorous convection containing graupel, the bright band is absent and the fall in Z with height is less marked. If accurate estimates of surface precipitation are to be made, based upon radar observations taken within or above the bright band, it is important to use a correction scheme which uses a different vertical profile of reflectivity (VPR) for the two precipitation types. Using a large radar data set, this work addresses the issue of VPR variability by constructing average vertical profiles and sorting them into snow and graupel categories using the value of the Linear Depolarization Ratio at the melting layer. These observations show that convection is often embedded within stratiform precipitation, and some convective showers containing snow have bright bands. As a result, the use of an average profile over the whole region scanned by radar leads to only marginal improvement in rain estimates. Instead, this work proposes that a bright band correction should always be applied unless the value of Z at 1.5 km above the bright band exceeds 30 dBZ, in which case a 'convective' vertical profile of -2 dBZ km^{-1} should be used. This Z threshold indicates that graupel only forms when the ice water content exceeds 0.35 gm^{-3} which has implications for ice parametrization schemes in mesoscale models.

KEYWORDS: Linear Depolarization Ratio Precipitation Vertical profile of reflectivity

1. INTRODUCTION

One of the major problems in using radar to estimate rainfall is that the lowest beam elevation can either overshoot the precipitation or intercept the enhanced reflectivity associated with melting snow (the 'bright band', BB). Joss and Waldvogel (1990) stated that the major source of error in rainfall rate estimation lay not in the often researched area of the relationship between radar reflectivity, Z, and rainfall intensity, R, but rather in the heterogeneous nature of the vertical reflectivity profile. If the beam encounters the BB, the rain rate will be overestimated by up to a factor of 5 at S-band and C-band; if Z is within the ice region above the BB, the surface precipitation at that pixel will be hugely underestimated.

Figure 1 shows a typical vertical reflectivity profile (VPR). Region A is populated by a mixture of ice particles and snow. Upon the onset of melting (region B), these snow flakes acquire a shell of liquid water which causes an increase in dielectric constant. As their size is retained during the early part of melting they appear to the radar to be giant raindrops, and because $Z \propto (\text{diameter})^6$, there is a dramatic increase in the reflectivity of some 7 to 13 dBZ; 5.8 dBZ due to the change in dielectric constant, the remainder to the large size of the wet snowflakes. The greater reflectivities have larger enhancements because the flakes are larger with lower densities. Fabry and Zawakski (1995) listed six effects which are in operation at the melting layer, each contributing to a greater or lesser extent to the enhancement of reflectivity. In addition to the change in dielectric constant they postulated that the increase in particle growth rate, terminal velocity, particle size distribution, particle shape and orientation could be important factors. They asserted that melting itself is not a sufficient condition to explain the shape and magnitude of the BB. However, they did not consider the large size of the wet snowflakes. Beneath the BB

* Corresponding author, present address: Plymouth Marine Laboratory, Prospect Place, Plymouth, Devon PL1 3DH, UK. e-mail: T.J.Smyth@pml.ac.uk.

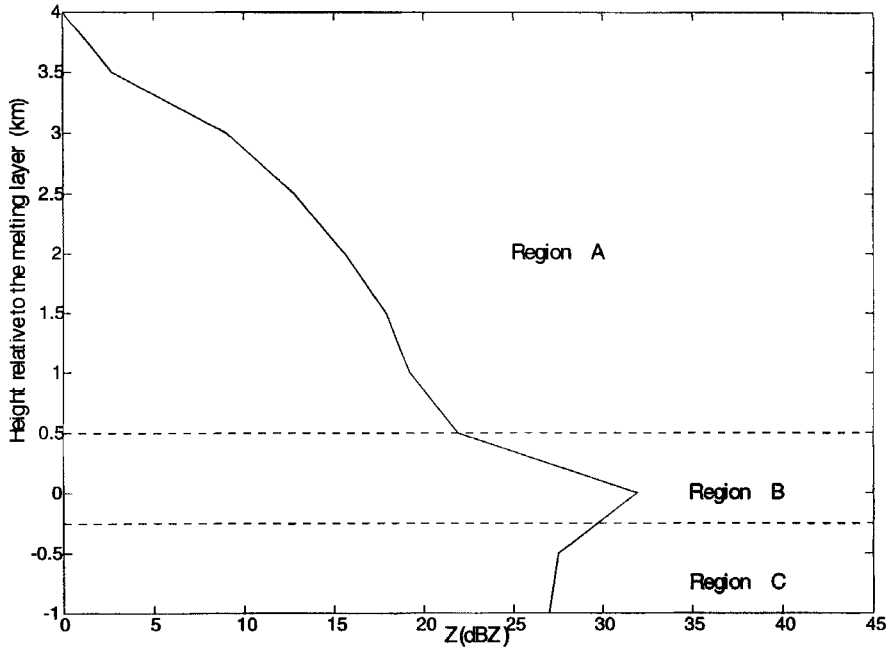

Figure 1. Typical vertical reflectivity profile for a shower containing snow. The various regions labelled are described in the text.

(region C) the increase in hydrometeor terminal velocity causes a reduction in the returned power as the concentration of raindrops is diminished.

In regions of vigorous convection the hydrometeors are higher-density graupel or soft hail and the BB is absent; but such areas are often surrounded by more stratiform precipitation which does have a BB. Any scheme to correct for the BB must be able to recognize convective cores. If the correction scheme is applied in error to such cores then the high-reflectivity regions of heavy precipitation, with the potential to cause flash floods, will be suppressed. The various schemes proposed to correct vertical profiles of reflectivity are reviewed in section 2. A polarization parameter which can identify the BB is introduced in section 3, and a Z threshold proposed which has the potential to distinguish between precipitation containing snow from that containing graupel. The implications of this for mesoscale cloud modelling are also discussed. A statistical analysis of vertical profiles of reflectivity with and without BBs is presented in section 4, and a new correction scheme is proposed in section 5.

The radar data used in this paper were obtained using the S-band ($\lambda = 9.75$ cm) Chilbolton radar which is situated in southern England. The radar has polarization capability, and a narrow (0.28°) beam width which allows excellent spatial resolution of precipitation events. Details of the hardware and engineering specifications of the radar can be found in Goddard *et al.* (1994).

2. Correction schemes

Precipitation overshoot is a problem particularly at middle to high latitudes in the winter (e.g. Harrold *et al.* 1974; Collier 1986; Joss and Waldvogel 1990). This is due to precipitation growth beneath the beam volume. Kitchen (1997) pointed out that over most of the land area in the UK the spacing of the operational networked radars is such that

the lowest radar beam is centred more than 1 km above sea level, and for 5% of the area the beam centre is more than 3 km in altitude. The freezing level is commonly below 1 km in winter (see Collier (1976) for a climatology) so, for complete radar coverage to be meaningful in terms of rainfall rate estimation, a correction to the overshooting beams (and the BB) is needed.

Several schemes have been advanced to solve this problem operationally. Collier *et al.* (1983) proposed the use of telemetering rain gauges; this approach yielded, on average, an improvement but was limited by the inherent lack of representivity provided by a limited number of rain gauges. Divjak (1994) used vertical profiles to correct for rainfall rate estimation in Italy. One of the problems that he encountered was the horizontal inhomogeneity of the precipitation. He calculated representative reflectivity profiles averaged over an area from 5 to 60 km around the radar and over a period of one hour. This representative profile was then divided into one of two classes: stratiform if the average Z gradient above the freezing level was above -2.5 dBZ km^{-1}, convective if it was less. The scheme resulted in a reduction of the overall spread of radar-to-raingauge ratios from a factor of 2.6 to 2.3. The disadvantage of this method is that the same profile is applied to the whole radar scan, even when (as is usually the case) the convective cells are embedded in stratiform precipitation. Andrieu and Creutin (1995) and Andrieu *et al.* (1995) propose a correction scheme for vertical profiles through an inverse solution applied to radar data from at least two elevation angles, but this technique still relies on the strong assumption of spatial homogeneity of the vertical profile.

One problem with using a vertical profile to correct for range is determining the representivity of the profile and its associated systematic and stochastic errors (Joss and Waldvogel 1989). Joss and Pittini (1991) extracted average vertical profiles every 10 minutes for a grid box of size 2×10^4 km^2. Comparing the radar estimates with rain gauges the difference in daily totals was reduced from a factor of 3 to a factor of 1.2. They found that even the use of climatological profiles improved the estimate of rainfall.

Kitchen *et al.* (1994) describe an operational scheme for vertical-profile correction using a detailed profile in which the BB enhancement is a function of reflectivity in the rain below, and has been derived from high-resolution (0.28° beamwidth) data obtained with the Chilbolton radar. This profile (Fig. 2) has a constant value of Z (Zb) in the rainfall; the BB enhancement of Z is represented by a triangular profile of depth 700 m and is related to Zb. Finally, the profile in the ice is fixed using the height of the top of the echo. The correction is performed by first normalizing the height of the profile so that the top of the BB coincides with the 0 °C isotherm derived from an operational forecasting model. The second step in the correction is to scale the Z values of the profile so that the observed value of Z from the lowest elevation radar beam agrees with the value obtained by multiplying the profile by the beam pattern of the radar at that range. Validation in stratiform rainfall showed a significant improvement in rainfall estimates.

The next step in improving the corrections would appear to be to use higher-elevation radar beams to provide a more accurate estimate of the Z gradient, rather than using a climatological profile. However, when this was done (Kitchen 1997) no further improvement could be detected in frontal rainfall, thus confirming the assertion of Fabry *et al.* (1992) that beyond the range where the radar horizon intercepts the freezing level "any attempt to obtain quantitative rainfall estimates is futile". It is interesting to note that for this very reason quantitative use of radar estimates of rainfall have often been limited to a range of 75 km.

An alternative approach is to compute the expected vertical profile of reflectivity from a detailed microphysical model of the melting snow (Hardaker *et al.* 1995). The advantage is that the appropriate profile can be computed using parameters, such as lapse rate and

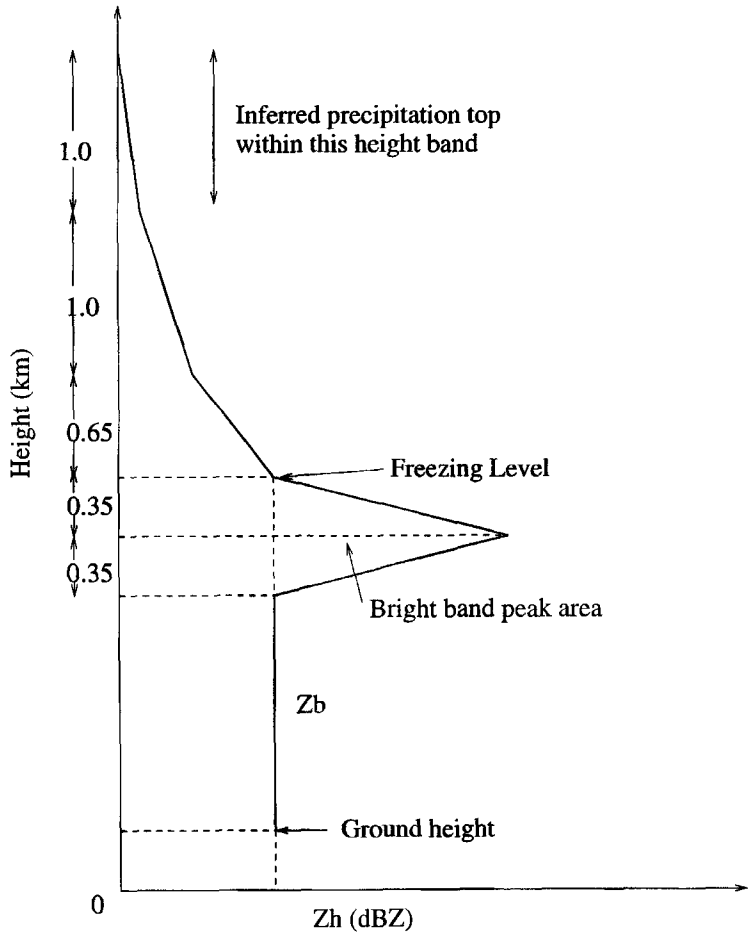

Figure 2. Idealized vertical profile of radar reflectivity, Zh, with approximate heights associated with various features, after Kitchen *et al.* (1994). Zb is radar reflectivity in the rainfall.

humidity profile at a particular time and place, derived from an operational mesoscale model. Our experience is that the computed profile is very sensitive to detailed assumptions of the melting process for snowflakes, such as the size of the wet core of the melting snowflake; a small error in this size has an enormous effect on the predicted reflectivity but the mesoscale model provides little guidance. Accordingly, it seems that the most accurate approach is to use the statistical variation of a large data set of observed profiles for various different conditions.

Allusion has already been made to the difference in vertical reflectivity between snow and graupel showers. Many authorities (e.g. Collier *et al.* 1983; Divjak 1994; Fabry and Zazwadski 1995) seek to discriminate between different types of precipitation in correction algorithms. In this paper distinction will be made between precipitation containing snow and that containing graupel.

TABLE 1. *LDR* LIMITS IN SNOW AND GRAUPEL

Shower type	*LDR* limits (dB)
Graupel	$-28 \leqslant LDR < -22$
Snow	$-18 \leqslant LDR < -12$

3. DISCRIMINATION BETWEEN SNOW AND GRAUPEL

The Linear Depolarization Ratio, *LDR*, is an excellent discriminator between melting graupel and melting snow. *LDR* is defined as:

$$LDR = 10 \log_{10} \frac{Z_{VH}}{Z_{HH}} \quad \text{(dB)}, \tag{1}$$

where Z_{HH} is the reflectivity both transmitted and received in the horizontal polarization, and Z_{VH} measures the depolarization from the vertically transmitted signal into the horizontal. *LDR* senses oblate-particle fall mode; values of *LDR* above the antenna limit of −32 dB occur for particles which cant or tumble as they fall. Because water has a higher dielectric constant than dry ice, oblate wet particles have higher values of *LDR*.

In the UK most convective showers have BBs accompanied by *LDR* values of about −16 dB (Frost *et al.* 1991), suggesting the presence of snow. In more vigorous showers there is no discernible BB in *Z*, and *LDR* values at the melting layer are typically −25 dB, indicative of graupel. These values are theoretically consistent (Figs. 1 and 2 in Frost *et al.*) with both types of ice tumbling randomly, but with wet snowflakes having an average axial ratio of about 0.5 to 0.6 whereas that of graupel pellets was about 0.8. Frost *et al.* later verified these shapes by using simultaneous aircraft flights. Table 1 shows the values of *LDR* used in this paper to discriminate between snow and graupel showers. It is possible for moderate to intense showers to contain both snow and graupel, the latter occurring within the updraught of the storm where riming rates are greatest and the former in the more stable regions of the cloud. *LDR* allows the small-scale distribution of the hydrometeors to be observed.

To study the difference between vertical reflectivity profiles from graupel and snow, the data points were extracted from vertical range–height indicator scans (RHIs) taken by the Chilbolton radar by splitting each scan into 3 gate (900 m) range 'bins'. For each bin the average reflectivity at various heights and *LDR* values at the melting layer were recorded. Averaging was carried out to allow for wind shear displacing the falling hydrometeors from a vertical path. Only data between 0 and 80 km from the antenna were used, as beam width spread leads to a loss in resolution at longer ranges. Figure 3(a) refers to a case study of 5 July 1991 when a line of severe convection embedded within stratiform rain, having its origins over the continent, approached Chilbolton from the south. The data set consists of 70 RHIs spread over a three-hour period. Figure 3(b) shows a random set for days with showery conditions covering 20 days and 38 separate RHIs. Data points to the right of the dashed line in Fig. 3 are indicative of snow. It shows convincingly that the 30 dBZ threshold 1.3 km above the BB is rarely exceeded in snow.

The 30 dBZ threshold 1.3 km above the melting layer in snow corresponds to a temperature of around −5 °C assuming a saturated adiabatic lapse rate (between −5 and −7 °C km^{-1}). This temperature could be significant for two reasons. Firstly, −5 °C is the temperature threshold which marks the acceleration in the rate of snowflake aggregation. This is due to adhesion between two colliding particles being increasingly likely above

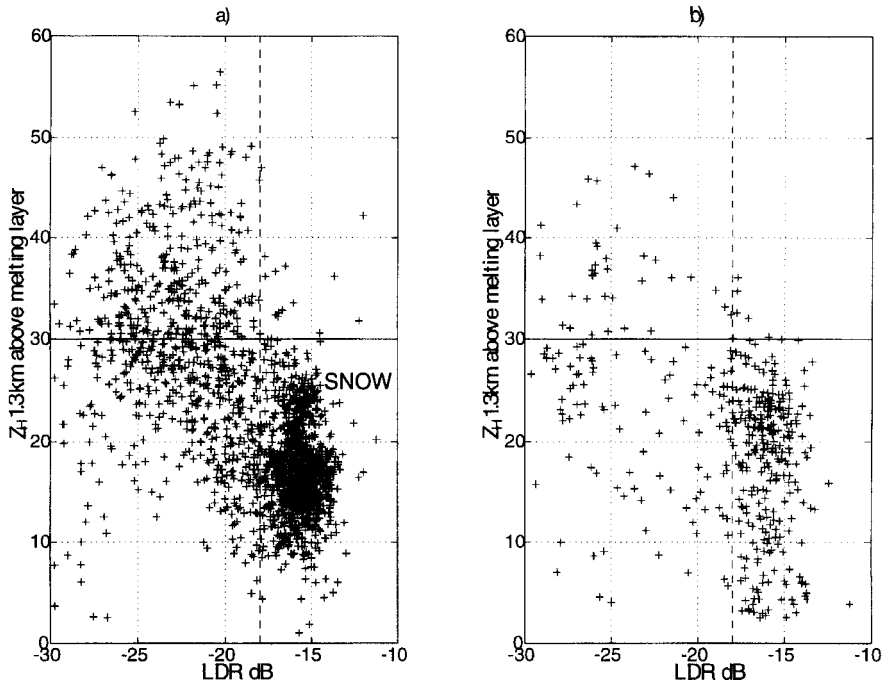

Figure 3. Linear depolarization ratio, LDR, against radar reflectivity, Z_H, at a height of 1.3 km above the melting layer for: (a) case study 5 July 1991, and (b) 20 days of showery precipitation. The solid line is the 30 dBZ threshold, and the dashed line is where the $LDR = -18$ dB. To the right of the dashed line precipitation contains snow above the melting layer; to the left graupel.

-5 °C (Wallace and Hobbs 1977). Put simply they become 'stickier'. Fabry and Zawadski (1995) also observed that 1.2 km above the BB top there was a considerable increase in Z. They attributed this to an increase in the magnitude of aggregation efficiency. Secondly, -5 °C marks the peak in the efficiency of the Hallet–Mossop ice-multiplication process (Hallet and Mossop 1974). Secondary ice splinters are produced as internal stresses break up frozen hydrometeors. Stewart *et al.* (1984), using probe measurements aboard an aircraft, found that the largest concentrations of ice crystals occurred at -5 °C. An increase in aggregation efficiency combined with an increase in the population of ice crystals will act to raise the value of the reflectivity, although the latter will contribute very little directly. A more important effect could be that more ice crystals will be made available for the aggregation process.

Graupel showers tend to have values of Z greater than 30 dBZ at this altitude. This is because graupel forms in the most vigorous section of convection. Graupel is formed by riming, a process which requires an updraught if frozen hydrometeors, such as a snowflake, are to encounter the necessary supercooled liquid water which freezes on impact. The most vigorous convective cells have a large updraught so that liquid water content (LWC) is high enough for graupel to form.

The Z threshold above the snow melting layer has important implications for modelling micro-physical processes, such as aggregation which is poorly understood and hence difficult to parametrize. The important governing factors in the aggregation process are the concentrations, sizes and densities of the ice particles. Using a combination of radar and coincidental aircraft micro-physical measurements (Thomason *et al.* 1995) it is possible to derive the size spectra and densities of the ice particles in a cloud and also infer

possible growth processes. Once the density is known, a general relationship for the ice water content, $IWC = f(Z)$, can be derived empirically. This is found to be (Thomason, personal communication):

$$IWC = 0.042Z^{0.31}, \tag{2}$$

where Z is in $\mathrm{mm^6 m^{-3}}$. Using (2), the Z threshold 1.3 km above the melting layer corresponds to an IWC of 0.35 $\mathrm{g\,m^{-3}}$. This IWC threshold value could prove a useful diagnostic for validating mesoscale cloud models, which now carry prognostic variables for the mixing ratio of different forms of ice such as snow and graupel. Some of these models may produce too much or too little graupel, which will in turn effect the precipitation rate and the LWC within the cloud. An example is given by Swann (1998) who used radiosonde data to initialize a cloud resolving model, and allowed convection to occur by warming the surface slightly. By comparing the model output with radar measurements made by the Chilbolton radar, the partitioning between the hydrometeors could be validated. Days were studied where either graupel or snow showers were detected by the radar (this being apparent by the return in LDR) and a corresponding radiosonde ascent used to initialize the model. As an experiment, the equation producing graupel by riming LWC was only switched on when the IWC exceeded the threshold of 0.35 $\mathrm{g\ m^{-3}}$. Without the threshold the model produces graupel when none was observed (see Swann (1998) for detailed results). The threshold has the effect of prescribing the value of snow mass concentration before snowflakes are converted to graupel via the process of riming liquid cloud (liquid water). These results show that more realistic modelling of clouds can be made using the IWC threshold for riming.

4. Analysis of VPRs

RHI scans from the Chilbolton data set were selected where both coincidental Z_H and LDR were recorded. The value of Z was sampled at prescribed heights relative to the melting layer, and a complete vertical profile constructed for every 300 m range gate between 0 and 80 km from the radar. The small spatial scale was used to enable resolution of the high-reflectivity cores. The height of the melting layer for moderate showers and stratiform precipitation was fixed for each separate range gate profile as the height where LDR was a maximum. This value was also used to characterize the vertical profile in terms of snow or graupel. The discrimination limits used are those shown in Table 1. Using this method to fix the melting layer height in severe convection is more problematic. Wet hail, forming at altitudes far above the melting layer, can give LDR returns typical of melting graupel or even snow, and result in spurious fixing of the melting layer height. Therefore, for the three days of severe convection studied, the melting layer height is not fixed automatically using the altitude of the maximum LDR return at each range gate profile. Rather it is fixed for the whole scan using the peak in the histogram of the height where LDR associated with melting graupel (or melting snow) is found. Once the LDR and Z data have been collected for each scan the vertical profiles are categorized in terms of the reflectivity 500 m below the melting layer. The value of Z at this altitude is taken to be representative of the reflectivity in the rain (Divjak 1994). The various profiles are sorted in their entirety into 5 dBZ interval 'rain bins' between 0 and 65 dBZ.

(a) *Stratiform*

Data were collected from 5 days of stratiform precipitation, consisting of 72 RHIs and 7892 vertical profiles. Stratiform precipitation was defined as having values of $LDR \geqslant -18$ dB (Frost *et al.* 1991) over a widespread region of the scan. Each RHI is separated

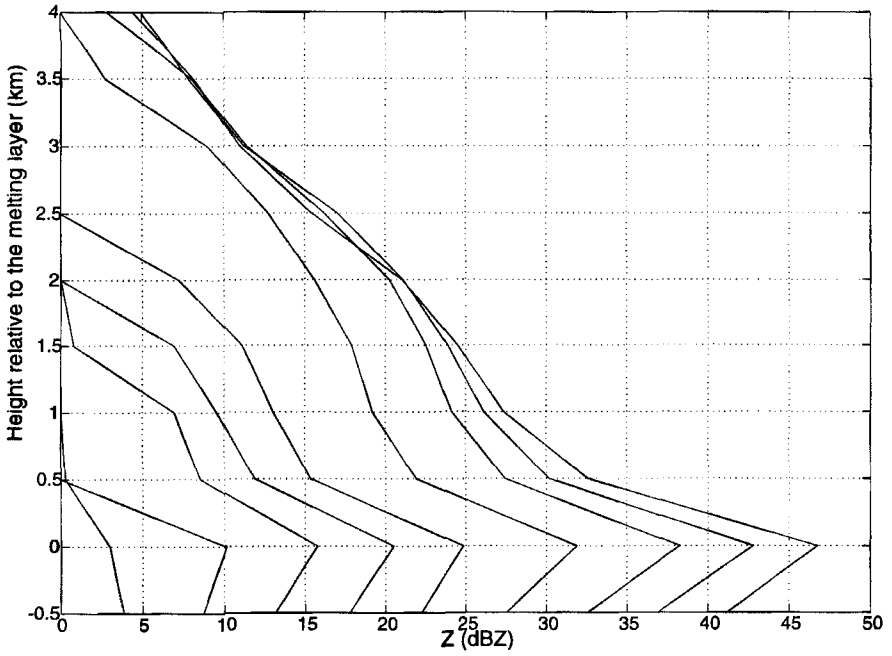

Figure 4. Median radar reflectivity, Z, profiles at height sampling intervals of 500 m for 5 dBZ rain intervals in stratiform precipitation.

by at least 4 minutes from any other in the data set. The results are presented to provide a comparison with the convective precipitation, and to lead to better formulation of BB removal algorithms when convection is active. Figure 4 shows the median reflectivity profiles for the data collected; the reflectivity is considered to be constant from 500 m below the BB to the ground. Several qualitative observations can be made. Firstly, the profiles contain snow above the melting layer, deduced from the values of LDR. This is hardly surprising as stratiform precipitation is characterized by gentle uplift of the order of a few cm s^{-1}, rather than the more vigorous ascent experienced in severe convection; the rapid riming of snow which leads to graupel formation requires high vertical velocities. Secondly, as Z increases in the rain there is a corresponding increase in the reflectivity slope above the BB. Fabry and Zawadski (1995) attributed this increased gradient with height above the freezing level to the increasing importance of aggregation compared with the mechanisms of accretion and deposition of water vapour. The latter two mechanisms are important at lower rain-reflectivities (0–10 dBZ). Figure 5 shows the standard deviations associated with the median reflectivity profiles for the 30–35 dBZ, 35–40 dBZ and 40–45 dBZ rain bins. These are the important profiles as they represent surface rainfall rates greater than 2.7 mm hr^{-1} and up to 23.7 mm hr^{-1}. The standard deviations are quite large and overlap considerably, especially at greater altitudes. This is shown clearly in Table 2. For example the standard deviation at 1.5 km above the melting layer for the 30–35 dBZ rain bin is ± 5 dBZ, which is a factor of ± 2 in terms of rainfall rate estimation. The overlap between the vertical profiles in terms of rainfall rate estimation would, at first sight, seem to preclude them for use in surface rainfall estimates. (It is unlikely that averaging over a greater number of gates, which would in effect simulate the radar response at a lower resolution, will reduce this noise). This would be consistent with the results of Kitchen (1997) where no marked improvement was found on applying an idealised vertical profile

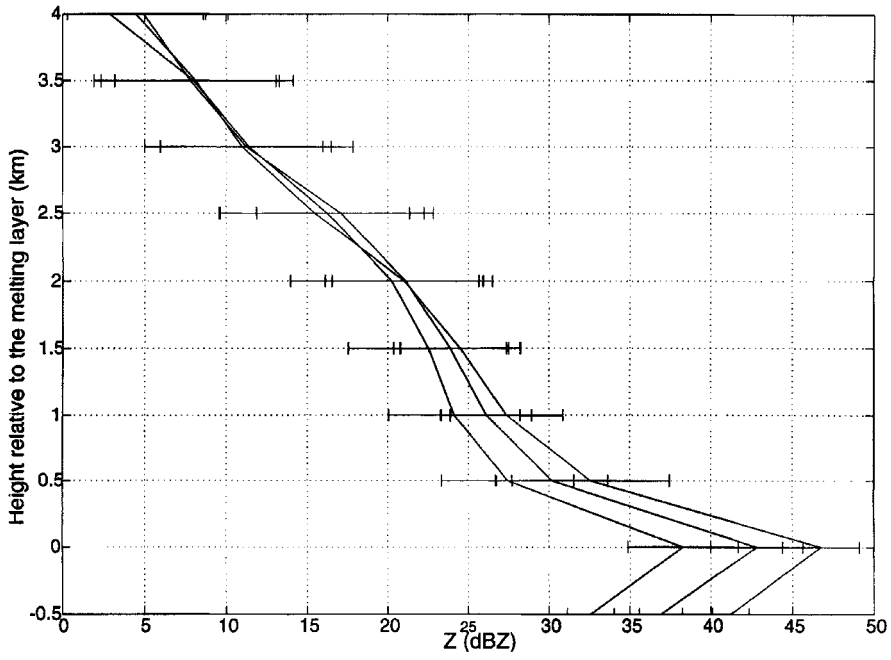

Figure 5. Standard deviations associated with the median radar reflectivity, Z, profiles for the 30–35, 35–40, 40–45 dBZ rain bins.

TABLE 2. STANDARD DEVIATIONS (std) FROM THE MEDIAN AT EACH HEIGHT ASSOCIATED WITH 5 dBZ WIDE RAIN BINS

Height relative to the melting layer (km)	30–35 dBZ median ± std	35–40 dBZ nmedian ± std	40–45 dBZ median ± std
−0.5	32.6 ± 1.5	36.9 ± 1.3	41.2 ± 1.1
0.0	38.3 ± 3.4	42.8 ± 2.8	46.7 ± 2.4
0.5	27.4 ± 4.1	30.2 ± 3.5	32.6 ± 4.9
1.0	24.1 ± 4.1	26.1 ± 2.8	27.4 ± 3.5
1.5	22.5 ± 5.0	23.9 ± 3.5	24.5 ± 3.7
2.0	20.3 ± 6.3	21.1 ± 4.6	21.0 ± 4.9
2.5	16.2 ± 6.6	17.0 ± 5.2	15.5 ± 5.9
3.0	11.4 ± 6.4	11.2 ± 5.3	11.0 ± 5.0
3.5	8.0 ± 6.1	7.8 ± 5.5	8.1 ± 5.0
4.0	2.9 ± 5.9	4.9 ± 5.2	4.5 ± 4.2

above the BB. The variability is too great at increasing altitude to allow the surface rainfall to be extracted, and a fixed value of Z at a certain height can diverge to several solutions. This can be shown by using Fig. 5 to make a few example calculations. Taking a reflectivity of 12 dBZ at a height of 3 km above the melting layer ($Z_{3\mathrm{km}}$) could feasibly result in the use of 3 median reflectivity profiles, namely the 30–35 dBZ, 35–40 dBZ and 40–45 dBZ rain bins, with their associated standard deviations at the surface. If the 'ground truth' (surface) reflectivity (Z_b) is assumed to be 37 dBZ then comparisons can be made with $Z_{3\,\mathrm{km}}$ and associated errors. To convert the value of Z into a rainfall rate (3) will be used:

$$Z = 200R^{1.6}. \tag{3}$$

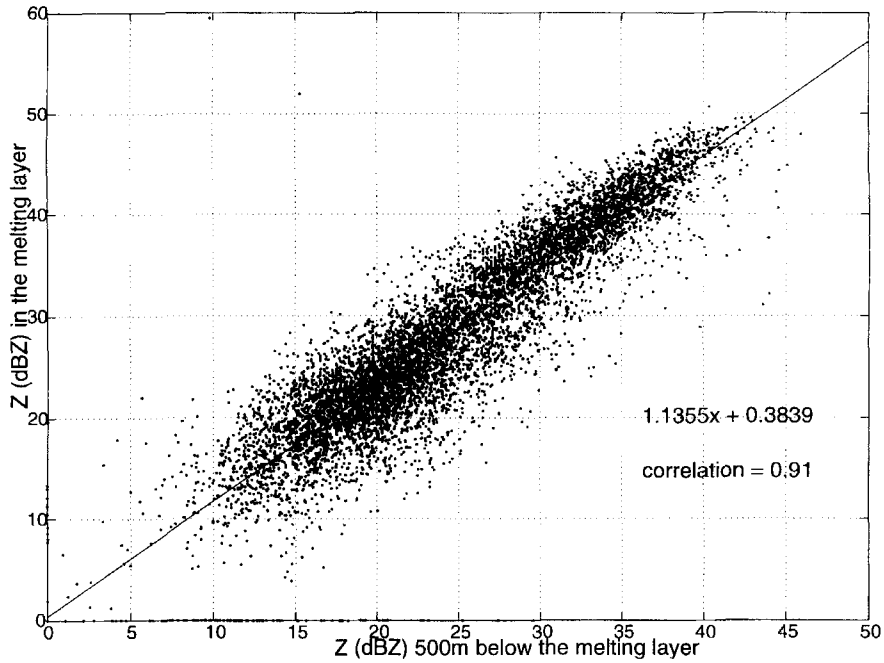

Figure 6. Linear fit between the radar reflectivity 500 m below the melting layer, Z_b, and in the melting layer, Z_{melt}, for stratiform precipitation.

Z_b and Z_{3km} are equivalent to rainfall rates of 8.0 mm hr^{-1} and 0.2 mm hr^{-1} respectively. In other words, the beam overshooting the precipitation to a height of 3 km above the melting layer will underestimate the rainfall rate by a factor of 40. If the vertical profiles were used to adjust for the precipitation overshoot this error could be considerably reduced. The surface value of Z (Z_b), given a value of Z_{3km} of 12 dBZ, would lie between 30 and 45 dBZ. This results in equivalent rainfall rates of 2.7 mm hr^{-1} and 23.6 mm hr^{-1} respectively. The error in the rainfall rate estimation would be reduced, therefore, from an underestimate by a factor of 40, to an under/overestimate by a factor of ± 3. This is still a considerable error when compared with the errors of about 40% associated with using a particular relationship of Z and R (Goddard and Cherry 1984). There is also an important additional problem of the beam spreading at greater ranges. For example if the beam width is 1° (a typical value) the beam will have spread to a depth of 1 km at a range of 60 km. This is twice the vertical resolution of the Z profile. The technique of multiplying a standard profile by beam width (Kitchen *et al.* 1994) overcomes this.

A simpler way of extracting Z_b is to produce a polynomial fit between the value of Z at various heights relative to the melting layer and Z_b. Figure 6 shows an approximately linear relationship between the value of Z at the melting layer (Z_{melt}) with Z 500 m below the melting layer height (Z_b). In Fig. 6 the enhancement in the melting layer is slightly underestimated, as Z_{melt} was the value of Z where LDR was a maximum, this was sometimes between 100 and 200 m different from the height of maximum Z. The correlation of 0.91 between the polynomial fit and the data suggests that there should be a great deal of benefit from implementing this scheme to reduce errors in rainfall rate estimation around the melting layer. Any benefit from using a polynomial fit is reduced with increasing altitude, as there is a considerable increase in the amount of data spread. This is shown by the reduction in the correlation coefficient. Table 3 shows the values of

TABLE 3. POLYNOMIAL FITS WITH ASSOCIATED CORRELATION COEFFICIENTS TO OBTAIN SURFACE REFLECTIVITY FROM VARIOUS HEIGHTS

Height relative to the melting layer (km)	α_0	α_1	Correlation
0	1.1	0.4	0.9
0.5	0.9	−4.0	0.8
1.0	0.8	−4.0	0.7
1.5	0.8	−5.6	0.7
2.0	0.8	−7.4	0.7
2.5	0.6	−7.5	0.6
3.0	0.5	−5.0	0.5
3.5	0.3	−3.4	0.4
4.0	0.2	−2.2	0.4

the polynomial (first order) coefficients, which are in the form of $\alpha_0 Z_b + \alpha_1$. At heights of 3.5 and 4 km above the melting layer the correlation coefficient drops to below 0.5, which means that no polynomial is of quantifiable use. Fortunately, the UK radar network spacing is sufficiently dense to allow most of the land surface area to be within 100 km from a radar. It is therefore unusual for the lowest elevation beam to overshoot the BB by more than 1.5 km. When the beam encounters ice at this elevation it still leads to an underestimation of the rainfall rate by about a factor of three (calculated from the 35–40 dBZ median profile, Fig. 5). However, when the rainfall rate is estimated using a multiple-beam method such as proposed by Kitchen (1997), then altitudes of 3.5 and 4 km are frequently encountered. Consider the worst-case scenario where the 0 °C isotherm is 500 m above the ground. The radar beam at elevation 1.5° would intersect 4 km in altitude (3.5 km above the melting layer) at a range of 115 km. This means that data from scans at elevations greater than 1.5° at the longest ranges, especially in the winter, are frequently at an altitude where disentangling of the surface rainfall rate is futile.

(*b*) *Moderate showers*

The data set of convective precipitation consists of 200 RHIs with 5312 profiles spread over 23 days. Three of the days covered exceptionally intense convective outbreaks (surface reflectivities exceeded 55 dBZ) and most of the data for these days will be covered in subsection (c). Figure 7 shows a comparison between the stratiform, and snow/graupel shower cases. The number of snow shower profiles is low, because showers by their very nature take up a smaller area than more widespread stratiform precipitation.

Comparing the snow shower profile with that of the stratiform precipitation, shows that the snow profile is steeper than that of the stratiform at altitudes greater than 1.5 km above the melting layer. (Although it must be noted that there is a severe deficit in the number of snow profiles in comparison with the number of stratiform.) This could be due to the increased *LWC* available in convective compared with stratiform clouds; typical values are 1.0 g m^{-3} and 0.1 g m^{-3} respectively.

The graupel vertical profile (which includes profiles from the severe convection cases detailed in subsection (c)) is more vertically homogeneous than both the stratiform and snow cases. The pronounced BB is absent. The increase in reflectivity caused by aggregation above the melting layer does not occur. This is because the graupel is physically different to dendrites which adhere together when they become entwined on impact. Graupel particles tend to rebound on impact due to their shape and density. Graupel is formed by the riming, rather than the aggregation, of ice crystals. Beneath the melting layer the

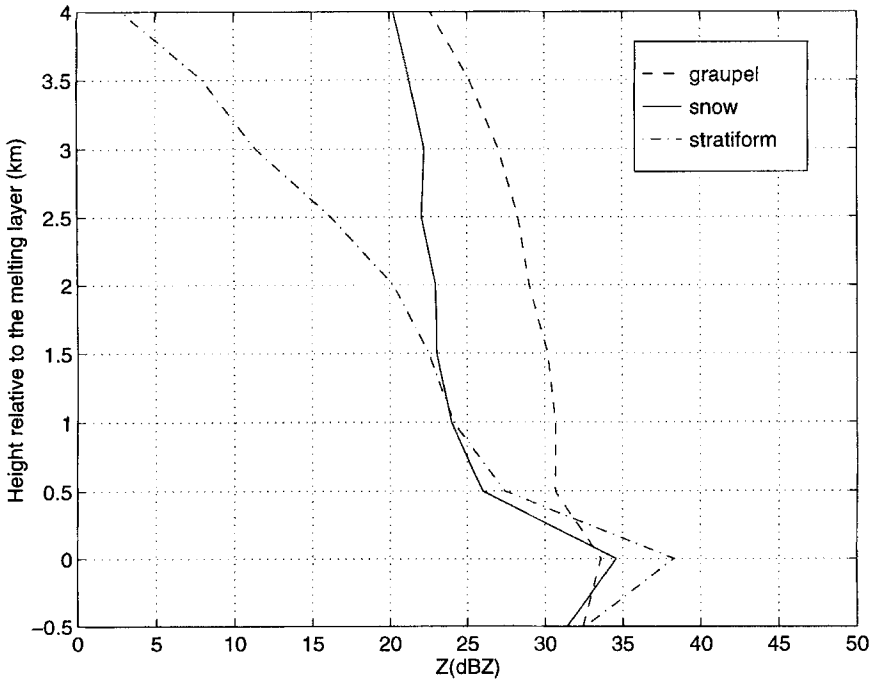

Figure 7. Comparison between 30–35 dBZ rain bin median vertical radar reflectivity, Z, profile for stratiform (1092 cases; dot dash line), snow showers (27 cases; solid line) and graupel showers (303 cases; dashed line). The frequency of snow showers exceeds that of graupel showers at lower rain-bins.

TABLE 4. STANDARD DEVIATIONS ASSOCIATED WITH EACH PRECIPITATION TYPE FOR THE 30–35 dBZ RAIN BIN MEDIAN VERTICAL PROFILE

Height relative to the melting layer (km)	Graupel ±	Snow ±	Stratiform ±
0	3.6	5.5	3.4
0.5	5.8	5.7	4.1
1.0	7.2	5.9	4.1
1.5	8.6	5.9	5.0
2.0	9.4	5.5	6.3
2.5	10.0	5.5	6.6
3.0	10.4	4.0	6.4
3.5	10.7	4.0	6.1
4.0	11.6	3.8	5.9

reflectivity decrease is not apparent to such an extent, because the terminal velocity of graupel (2.5 m s^{-1}) is greater than that of snow ($\sim$1 m s^{-1}) and the size of wet graupel is similar to that of a raindrop. This could mean that graupel is surviving in its frozen state further beneath the BB.

Table 4 shows that although the median profile is more vertically homogeneous than that associated with snow, there are large standard deviations associated with each data point. Part of this could be due to the small-scale structure of graupel regions in a convective cell, typical dimensions being 5 km in diameter. Another factor could be the growth and decay of graupel showers, and their associated precipitation falling out rapidly compared

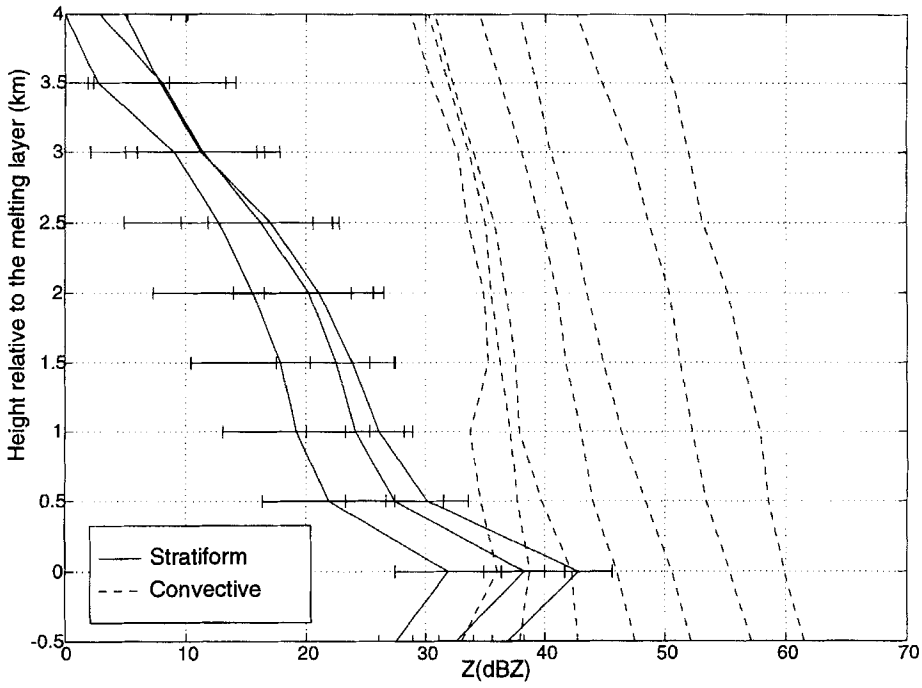

Figure 8. Contrast between vertical radar reflectivity, Z, profiles in severe convection (dashed) and stratiform (solid) situations. The graupel profile in Fig. 7 includes data from the severe convection cases.

with aggregates. Most of the standard deviation quoted for the graupel showers is as a result of the most vigorous convective cells. The updraughts can be so vigorous as to result in a 'top heavy' reflectivity profile; in other words the reflectivity aloft is greater than that at the ground. This can be caused by hail forming in the icing regions of the cloud. Fortunately these profiles are short lived as the hail quickly descends by virtue of its large terminal velocity, which may be of the order of 30 m s^{-1} for large hail.

(*c*) *Severe convection*

The data set for the strongly convective cases was collected on three separate days. During these storms the precipitation consisted of heavy rain and hail which was reported at several locations. Figure 8 shows the contrast between strong convection and stratiform precipitation classified by LDR. The profiles categorized in the strong convection section were all found to have graupel at the melting layer, using the value of LDR. As in the comparison between the stratiform and moderate showers, the BB is absent for the showers containing graupel. The reflectivity field is very much more vertically homogeneous than is the case for stratiform precipitation, and the reflectivities are much more intense to greater altitudes. The major difference occurs above the melting layer. The stratiform profiles decrease rapidly with height, in the magnitude of Z, whereas in the convective cells the gradients are somewhat less. This can be seen by comparing Tables 5 and 6. The stratiform first-order polynomials show an increase in the negative gradient (α_0) with increasing rain rate; this is matched by a corresponding increase in the correlation between the fit and the data. The convective data set, however, has a negative gradient ~ -2 dBZ km^{-1} for all rain rate intensities. This implies that individual gradients cannot be used to ascertain the value of Z_b in convective cases. The trend is more marked in stratiform cases, but again

TABLE 5. POLYNOMIAL FITS FOR STRATIFORM DATA POINTS BETWEEN 0.5 AND 4 km ABOVE THE MELTING LAYER OF THE MEDIAN VERTICAL Z PROFILE IN EACH RAIN BIN

Rain-bin (dBZ)	α_0	α_1	Correlation	Number of profiles
0–5	−0.1	0.1	0.6	22
5–10	0	0	–	90
10–15	−2.3	7.2	0.8	547
15–20	−3.6	11.7	0.9	1447
20–25	−5.1	17.3	0.94	1461
25–30	−6.3	26.6	0.98	1038
30–35	−6.9	32.1	0.99	1092
35–40	−7.4	34.4	0.99	723

TABLE 6. POLYNOMIAL FITS FOR CONVECTIVE DATA POINTS BETWEEN 0.5 AND 4 km ABOVE THE MELTING LAYER OF THE MEDIAN VERTICAL Z PROFILE IN EACH RAIN BIN

Rain-bin (dBZ)	α_0	α_1	Correlation	Number of profiles
15–20	−2.5	43.6	0.7	6
20–25	1.3	36.4	0.6	13
25–30	−1.9	37.4	0.7	63
30–35	−1.6	36.6	0.9	232
35–40	−2.1	39.3	0.98	580
40–45	−2.4	41.1	0.98	804
45–50	−2.7	45.8	0.99	846
50–55	−3.0	49.5	1.0	625
55–60	−3.0	55.6	0.99	385
60–65	−2.9	60.6	1.0	138

the differences are so small between the relative profiles as to render any extraction of the surface rainfall rate impossible. Clearly, any correction scheme would have to take account of the different vertical Z structure of graupel showers compared with stratiform precipitation and snow showers, otherwise over-correction will occur. This will be most pronounced in severe convection.

Figure 8 shows that at altitudes over 1 km above the melting layer 30 dBZ is not exceeded in the stratiform precipitation. If values greater than 30 dBZ are encountered above the melting layer then the convective profiles should be used to correct for precipitation overshoot.

5. BRIGHT BAND CORRECTION SCHEME

The BB correction scheme devised by Kitchen *et al.* (1994) relies on the measurements of Z at the lowest-elevation beam and the distance from the BB to the precipitation top, H. The code iterates until the modelled profile, multiplied by the radar beam width, gives the observed Z. The scheme has a choice of four possible profiles depending upon H. The profile scales as a background value of Z, Z_B i.e. Z in the rain. This is adjusted until Z_B gives the observed Z when the lower beam is multiplied by the profile.

An equivalent algorithm using the Chilbolton data does not require an iterative step, as the beam width is very narrow (0.28°). In heavy rain the top of the precipitation is more than 4 or 5 km above the BB. Using Fig. 4 from Kitchen *et al.* (1994), Z in the rain (Z_b) can

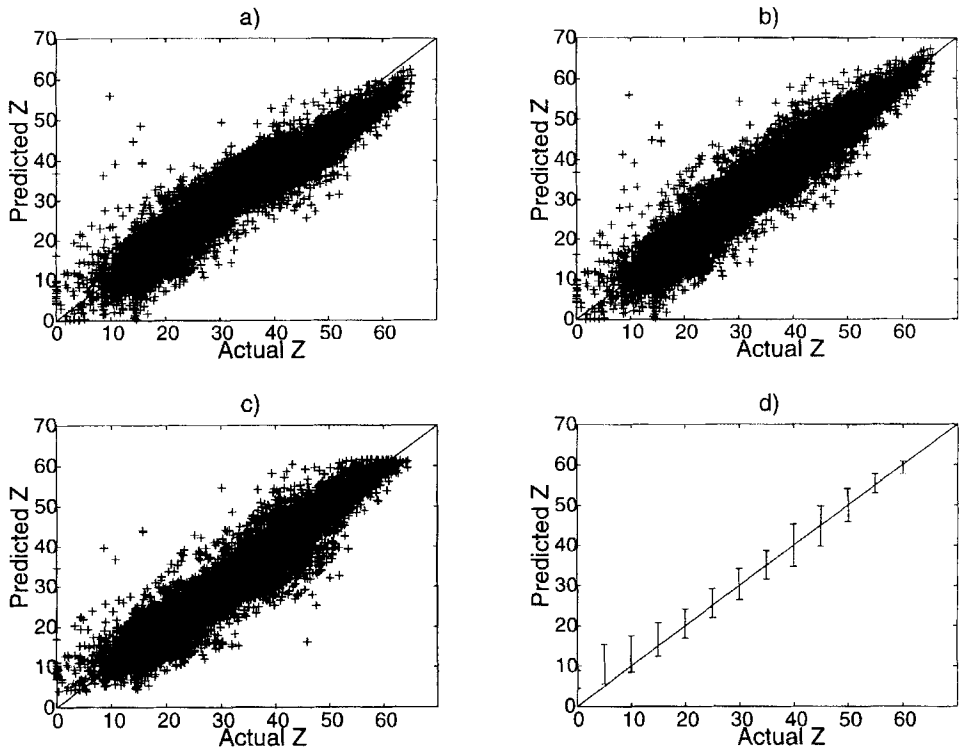

Figure 9. Predicted vs actual radar reflectivity, Z, 500 m below the melting layer (Z rain in text). (a) Kitchen *et al.* (1994); subtracting 5 dBZ from Z in the bright band (Z_{bb} in text). (b) Using Z threshold 1.5 km above the bright band. (c) Using median profiles. (d) The standard deviations associated with median profiles.

be approximated by subtracting 5 dBZ from Z in the BB (Z_{bb}). This is nearly equivalent to the relationship between Z_{bb} and Z_b derived from the vertical profiles in Fig. 8.

Both the stratiform and convective data sets collected were merged together and then used in the schemes described below. Scheme 1 is a direct implementation of the Kitchen *et al.* (1994) algorithm for a narrow-beam radar, and it implicitly assumes that all the profiles are stratiform in nature and that the value of Z at the melting layer height is always greater than Z_b. This is not the case for convective storms. Figure 9(a) shows that the scheme needs to be modified for strongly convective cases. The data points in this region deviate significantly away from the line representing equality between the predicted and measured values of Z. Another relationship needs to be derived for strongly convective cases. A threshold value of $Z = 30$ dBZ, this time set to 1.5 km above the BB, was used to delimit between the snow and graupel profiles. This has been used in scheme 2. If the threshold is exceeded, then 1.45 dBZ is added to the value of Z_{bb}; if not, then 5 dBZ is subtracted from Z_{bb} as in scheme 1. The value of 1.45 dBZ was obtained by finding the average value of the enhancement of Z between the melting layer height and the rain from the median profiles. Comparing Figs. 9(a) and (b) a marked improvement is shown in the accuracy of the predicted values of Z at higher reflectivities. The correlation coefficient between the actual and predicted value of Z_b, increases from 0.94 to 0.95 upon the addition of the threshold. This could be unrepresentative of the total improvement as it is in the higher, more data sparse, values of Z where the difference is made. The improvement at higher values of Z is also shown in Table 7. The figures were calculated by putting the data

TABLE 7. COMPARISON OF THE ACTUAL COMPARED WITH THE PREDICTED Z VALUE FOR 1 dBZ WIDE BINS

Actual (dBZ)	Scheme 1. (dBZ)	Scheme 2. (dBZ)	Scheme 3. (dBZ)
10	8.1 ± 7.2	8.1 ± 7.2	13.0 ± 4.5
20	18.3 ± 4.4	18.5 ± 4.6	20.6 ± 3.6
30	30.2 ± 3.6	31.0 ± 4.1	30.3 ± 3.9
40	37.0 ± 3.3	41.3 ± 4.7	40.0 ± 5.3
50	43.8 ± 3.3	49.8 ± 3.9	50.0 ± 4.1
60	53.4 ± 1.9	59.9 ± 1.9	59.3 ± 1.6

See text for descriptions of schemes 1–3.

points into 1 dBZ wide 'bins' based on the actual measured value of Z_b, and the mean and standard deviation calculated for the predicted Z_b. There is no improvement at the lower values of Z_b, which is to be expected, but at values of $Z_b \geqslant 30$ dBZ there is an increasingly marked difference between the two schemes.

Scheme 3 was developed along these lines, but this time median profiles were used to predict the value of Z_b. Two look-up tables of median profiles were constructed from the data sets of convective and stratiform precipitation. The look-up table profiles were categorized into being stratiform or convective by the value of LDR at the BB, the convective profiles being associated with graupel and stratiform profiles with snow. Therefore, the stratiform profile look-up table will categorize snow showers along with stratiform precipitation. A selection of the median profiles can be seen in Figs. 4, 5 and 8. The threshold value of $Z = 30$ dBZ, 1.5 km above the melting layer, was used to decide which look-up table to use. If this threshold was exceeded then the convective median profiles were used, otherwise the stratiform profiles utilized. From an operational perspective, the height of the BB can be fixed using the output from the mesoscale model.

Scheme 3 used the measured value of Z_{bb} to predict, via the relevant look-up table, the value of Z_b. It is a considerable improvement on scheme 1 at all but the very lowest values of Z. The improvement over scheme 2 is more marginal, most improvement being seen between 20 and 50 dBZ. These values of Z are most often observed in moderate to intense rainfall, and therefore scheme 3 should be implemented in preference to the others. The correlation coefficient between the predicted and measured values of Z is 0.95. The standard deviations from each of the three schemes are all very similar as this reflects the natural variability of the profiles rather than a particular scheme's accuracy.

Both schemes 2 and 3 show the importance of being able to delimit between convective and stratiform precipitation in terms of the surface reflectivities and consequently rainfall rates. The scheme of Kitchen *et al.* (1994) would considerably underestimate the value of Z_b in the presence of strong convection; there is some evidence of this occurring in practice. This can be overcome by use of the $Z = 30$ dBZ threshold, 1.5 km above the BB, to delimit between the two precipitation types. Scheme 3 is able to distinguish between snow and graupel implicitly without the need for LDR. Within scheme 3 a convective or stratiform median vertical profile is fitted by virtue of the value of Z, 1.5 km above the melting layer alone. This means that the scheme, using the LDR derived look-up tables, can be implemented operationally on radars which have no polarization capabilities.

For an operational radar the errors may well be less than those quoted in Table 7, which were derived from profiles with a 300 m gate resolution; averaging over greater distances could remove some of the small-scale variability introduced, for example, by wind shear.

On 12 August 1996 the UK networked radar at Chenies, situated in the Chiltern Hills to the north of London, observed a severe convective storm over Folkestone, some 120 km away. The lowest beam of the radar intercepted the storm at a height where the mesoscale model was predicting that the BB should be present. This led the automated radar adjustment to 'correct' for the high values of reflectivity (~50 dBZ) that were observed, as if the precipitation was stratiform in nature (M. Kitchen, personal communication). This led to a considerable underestimate of the rain rate that was experienced at the surface, this being verified by cumulative raingauge totals beneath the storm.

Clearly the adjustment to the reflectivity should not have occurred in this case; a vertical profile consistent with severe convection should have been utilized instead of one designed for use in winter stratiform precipitation. The mistake could have been eliminated if Z from other elevations had been used and a vertical profile of the storm built up.

6. Conclusions

The vertical reflectivity profiles for graupel showers, and particularly those in severe convection, differ considerably from those found in snow showers and stratiform precipitation. A threshold in reflectivity of 30 dBZ, 1.3 km above the BB, can potentially be used to delimit between snow and graupel showers. A BB correction scheme was devised to make use of this threshold and the inherent differences between the Z profiles of snow (stratiform) and graupel (convective). The median profiles were derived using the polarization radar data from Chilbolton, but have the potential for use on any radar which employs Z alone. The precipitation was categorized into graupel or snow by the value of Z, 1.5 km above the melting layer, and the value of Z in the rain predicted using an appropriate vertical profile. Schemes which were able to distinguish between precipitation containing graupel and that containing snow gave improved estimates of the surface reflectivities, especially when $Z_b \geq 30$ dBZ.

The use of two different correction profiles dependent upon the value of Z 1.5 km above the BB, appears to identify regions of embedded convection far more efficiently than the use of average profiles over a whole scan. The correction scheme proposed should reduce rainfall estimates when BB contamination is occurring, whilst also faithfully detecting the heavy rainfall associated with graupel in convective cores. The reflectivity threshold implies that graupel is only present when the IWC exceeds 0.35 g m^{-3}, and could be used in mesoscale models as a constraint in formulating equations for the riming of snow and also as a model validation tool.

Acknowledgements

This work was supported by the Natural Environment Research Council 'HYREX' grant GST/02/718. We thank the Radio Communications Research Unit group at Rutherford Appleton Laboratory for allowing access to the Chilbolton radar. Special thanks go to Malcolm Kitchen at the UKMO for helpful comments and for testing the bright band removal scheme on the C-band radar network.

References

Andrieu, H. and Creutin, J. D. 1995 Identification of vertical profiles of radar reflectivities for hydrological applications using an inverse method. I: Formulation. *J. Appl. Meteorol.*, **34**, 225–239

Andrieu, H., Delrieu, G. and Creutin, J. D. 1995 Identification of vertical profiles of radar reflectivities for hydrological applications using an inverse method. II: Sensitivity analysis and case study. *J. Appl. Meteorol.*, **34**, 240–259

Collier, C. G. 1976 The height of the freezing level during rainfall over the British Isles. *Meteorol. Mag.*, **105,** 381–392

1986 Accuracy of rainfall estimates by radar. I: Calibration by telemetering rainguages. *J. Hydrol.*, **83,** 207–223

Collier, C. G., Larke, P. R. and May, B. R. 1983 A weather radar correction procedure for real-time estimation of surface rainfall. *Q. J. R. Meteorol. Soc.*, **109,** 589–608

Divjak, M. 1994 Radar measurement of precipitation: The use of vertical reflectivity profiles. Pp. 73–84 in *Cost 75: Weather radar systems*. EUR 16103, European Commission, Brussels, Belgium

Fabry, F. and Zawadski, I. 1995 Long-term radar observations of the melting layer of precipitation and their interpretation. *J. Atmos. Sci.*, **52,** 838–851

Fabry, R., Austin, G. L. and Tees, D. 1992 The accuracy of rainfall estimates by radar as a function of range. *Q. J. R. Meteorol. Soc.*, **118,** 1427–1463

Frost, I. R., Goddard, J. W. F. and Illingworth, A. J. 1991 'Hydrometeor identification using cross polar radar measurements and aircraft verification'. Pp. 658–661 in Proceedings of the 25th Conference on Radar Meteorology, Paris. American Meteorological Society, Boston, USA

Goddard, J. W. F. and Cherry, S. M. 1984 The ability of dual polarisation radar (copolar linear) to predict rainfall rate and microwave attenuation. *Radio Sci.*, **19,** 201–208

Goddard, J. W. F., Eastment, J. D. and Thurai, M. 1994 The Chilbolton advanced meteorological radar: a tool for multidisciplinary research. *Electron. & Commun. Eng. J.*, **6,** 77–86

Hallet, J. and Mossop, S. C. 1974 Production of secondary ice crystals during the riming process. *Nature*, **249,** 26–28

Hardaker, P. J., Holt, A. R. and Collier, C. G. 1995 A melting layer model and its use in correcting for the bright band in single polarization radar echoes. *Q. J. R. Meteorol. Soc.*, **121,** 495–525

Harrold, T. W., English, E. J. and Nicholass, C. A. 1974 The accuracy of radar-derived rainfall measurements in hilly terrain. *Q. J. R. Meteorol. Soc.*, **100,** 331–350

Joss, J. and Pittini, A. 1991 'The climatology of vertical profiles of radar reflectivity to improve estimates of precipitation.' Pp. 828–831 in Proceedings of the 25th Conference on Radar Meteorology, Paris, France. American Meteorological Society, Boston, USA

Joss, J. and Waldvogel, A. 1989 'Precipitation estimates and vertical reflectivity profile corrections'. Pp. 682–688 in Proceedings of the 24th Conference on Radar Meteorology, Tallahasse, Florida. American Meteorological Society, Boston, USA

1990 Precipitation, measurement and hydrology, a review. Pp. 577–606 in *Radar in Meteorology: First edition*. Ed. D. Atlas. American Meteorological Society, Boston, USA

Kitchen, M. 1997 Towards improved radar estimates of surface precipitation. *Q. J. R. Meteorol. Soc.*, **123,** 145–163

Kitchen, M., Brown, R. and Davies, A. G. 1994 Real-time correction of weather radar for the effects of bright band, range and orographic growth in widespread precipitation. *Q. J. R. Meteorol. Soc.*, **120,** 1231–1254

Stewart, R. E., Marwitz, J. D., Pace, J. C. and Carbone, R. E. 1984 Characteristics through the melting layer of stratiform clouds. *J. Atmos. Sci.*, **41,** 3227–3237

Swann, H. 1998 Sensitivity to the representation of precipitating ice in CRM simulations of deep convection. *Atmos. Res.*, **48,** 415–435

Thomason, J. W. G., Illingworth, A. and Marecal, V. 1995 'Density and size distribution of aggregating snow particles inferred from coincidental aircraft and radar observations.' Pp. 127–129 in Proceedings of the 27th Conference on Radar Meteorology, Vail, Colorado. American Meteorological Society, Boston, USA

Wallace, J. M. and Hobbs, P. V. 1977 *Atmospheric Science an Introductory Survey*. Academic Press, New York